

A Construction of an Effective Hamiltonian from Feynman Diagrams : Application to the Light-Front Yukawa Model

Yuki YAMAMOTO*

Department of Physics, Kyushu University, Fukuoka 812-8581, JAPAN

Abstract

We study a similarity transformation to construct an effective Hamiltonian systematically, which does not contain particle-number-changing interactions, by means of Fukuda-Sawada-Taketani-Okubo's method. We show that such Hamiltonian can be constructed from Feynman diagrams and give rules for constructing it in the Light-Front Yukawa model. We prove that it is renormalized by the familiar covariant perturbative renormalization procedure. It is very advantageous that the effective Hamiltonian can be obtained from our rules *immediately*. We also numerically diagonalize it to the second order in the coupling constant as an exercise.

* E-mail: yuki1scp@mbox.nc.kyushu-u.ac.jp

§1. Introduction

For many years, the bound state problem for QCD has been studied very well but has not come to the complete understanding until today. The main difficulty is that the low energy dynamics of QCD needs nonperturbative calculations. One of the convenient tools to solve the problem is a Hamiltonian approach in Light-Front (LF) field theory which is quantized on the equal LF time surface.

An important feature of the LF field theory is that the vacuum is trivial; the Fock vacuum of the free part of the Hamiltonian is the true one. It is very useful in the relativistic bound state problem because we do not need to worry about solving the complex vacuum in contrast to the usual equal-time (ET) field theory. Even though the vacuum is trivial, to solve the Schrödinger equation for the relativistic bound state is difficult because it is natural that the eigenstates are constructed by the superposition of an infinite number of particle states allowed by symmetries of the Hamiltonian. Tamm-Dancoff (TD) approximation,¹⁾ which truncates the Fock space, that is, limits the number of particles concerned with the interaction, simplifies the practical calculations. While TD approximation was originally proposed in the ET field theory, Perry, Harindranath, and Wilson suggested a LF version of it.²⁾ They pointed out that since the truncated states do not consist a complete set of the Hamiltonian, ultraviolet (UV) divergences are nonlocal and noncovariant, and counterterms which should cancel the divergences depend on the sector of the Fock space within which they act. This is called the problem of “sector-dependent counterterms”.

A similarity transformation of the Hamiltonian does not change the eigenvalues and is useful for getting the effective Hamiltonian. There are two types of it. One is the transformation in momentum space, which is equivalent to integrating out states which exchange energies more than some energy cutoff, proposed by Głazek and Wilson,³⁾ and independently by Wegner.⁴⁾ It is interesting that it gives the nonperturbative low energy physics and a logarithmic confining potential in LF QCD,⁵⁾ although it is hard to get the effective Hamiltonian even in the lowest order in the coupling constant. The details of this method and applications are discussed in Ref. 6) and recent progress is seen in Ref. 7).

Another is the transformation in the particle number space, which reduces the Hamiltonian to one which has no particle-number-changing interactions so that the transformed one can be solved easily, and was proposed by Harada and Okazaki.⁸⁾ It can avoid the problem of sector-dependent counterterms because the origin of it is the general property of the Hamiltonian that it has particle-number-changing interactions and its eigenstates need an infinite number of particles. But its actual calculations are complicated and tedious. Although their method was considered in the LF field theory, it is not new in the ET context and has been

used for getting the TMO potential of nuclei.⁹⁾ We call it Fukuda-Sawada-Taketani-Okubo's (FSTO's) method.^{10), 11)} This method gives us an easier way for constructing the effective Hamiltonian and seems to be promising in the LF framework. However, it lacks manifest Lorentz covariance, and therefore it is difficult to tell what sort of divergences the effective Hamiltonian has before doing actual calculations. It makes the renormalization procedure more complicated than the usual covariant perturbation theory. It is highly desired to make transparent how the divergences emerge in the FSTO's framework.

The purpose of this paper is to show that the effective Hamiltonian constructed by the FSTO's method can be *immediately* obtained from Feynman diagrams as the S-matrix element can be in the covariant perturbation theory, and that one can use the usual renormalization procedure to renormalize it. It makes the construction of the effective Hamiltonian systematic and easier. Especially, it allows us to perform higher order calculations.¹²⁾

Our strategy is the following. First, we show that the FSTO's effective Hamiltonian is a sum of the auxiliary operator G and its products to the fourth order of the interaction part of the Hamiltonian. The advantages of using G are that it is constructed by the same Feynman diagrams as those for S-matrix elements, and that it has no particle-number-changing interaction so that one can easily calculate normal-ordering of the products of those. We give the rules for constructing G from Feynman diagrams. They are a little bit differ from the familiar Feynman rules in the covariant perturbation theory. The set of those rules is one of the main results of the present paper. Our method is more convenient and powerful for constructing the effective Hamiltonian and discussing the renormalization of it than the other similarity methods. Then, we find that there are three types of UV divergence. One is the familiar loop divergence which can be renormalized by the usual renormalization procedure. The second comes from the difference between our construction rules and Feynman ones. We can make it harmless by using an ambiguity. The above two only emerge in G . The last emerges from the products of the renormalized G 's. We show that it works as a box counterterm,¹³⁾ which is needed to cancel the cutoff dependence of the eigenvalue, in diagonalizing the effective Hamiltonian.

This paper is organized as follows. In Sec. 2, we briefly review the FSTO's method. In Sec. 3, we show that the effective Hamiltonian constructed from the FSTO's method is written in terms of the auxiliary operators F or G . F is written in terms of G . We consider the LF Yukawa model,¹³⁾ in which Lagrangian and Hamiltonian are given in Appendix A, as a concrete example, and give the rules for the construction of G from Feynman diagrams and how to renormalize it and the effective Hamiltonian. In Sec. 4, we summarize and discuss the validity of our method. In Appendix B, as an exercise, we calculate the eigenvalue of the ground states of the effective Hamiltonian up to the second order in the coupling constant in

the LF Yukawa model. In Appendix C, we explain an ambiguity of the energy integrations.

§2. Review of the FSTO's method

This section briefly reviews the FSTO's method partly following Ref. 11). The FSTO's method is to reduce a Hamiltonian to the block-diagonal form using a similarity transformation. We can get the effective Hamiltonian for the subspace of the Fock space without a loss of the necessary information.

We want to solve the Schrödinger equation

$$H|\Psi\rangle = E|\Psi\rangle, \quad (2.1)$$

for the second-quantized Hamiltonian H which consists of the free part H_0 and the interaction part H' :

$$H = H_0 + H'. \quad (2.2)$$

The eigenstate $|\Psi\rangle$ can be expanded by the complete set of H_0 . To divide the Fock space into two, we introduce a projection operator η which commutes with H_0 :

$$\begin{cases} \eta|\Psi\rangle = |\psi_1\rangle, \\ (1-\eta)|\Psi\rangle = |\psi_2\rangle, \end{cases} \quad (2.3)$$

where both $|\psi_1\rangle$ and $|\psi_2\rangle$ are the states written in terms of the eigenstates of H_0 . $|\psi_1\rangle$ is the state in the target Fock space at our disposal. For our purpose, we restrict η to the one which selects the states with definite number of particles. In the matrix notation, η and $|\Psi\rangle$ are written as

$$\eta = \begin{pmatrix} 1 & 0 \\ 0 & 0 \end{pmatrix}, \quad |\Psi\rangle = \begin{pmatrix} |\psi_1\rangle \\ |\psi_2\rangle \end{pmatrix}, \quad (2.4)$$

respectively, and we express an arbitrary operator O as

$$O = \begin{pmatrix} O_{11} & O_{12} \\ O_{21} & O_{22} \end{pmatrix}, \quad \begin{aligned} O_{11} &= \eta O \eta, & O_{12} &= \eta O (1-\eta), \\ O_{21} &= (1-\eta) O \eta, & O_{22} &= (1-\eta) O (1-\eta). \end{aligned} \quad (2.5)$$

Let us consider the similarity transformation that leads the Hamiltonian to the block-diagonal form in the following way

$$\mathcal{U}^\dagger H \mathcal{U} \begin{pmatrix} |\psi_1\rangle' \\ |\psi_2\rangle' \end{pmatrix} = \begin{pmatrix} H_{\text{eff}} & 0 \\ 0 & * \end{pmatrix} \begin{pmatrix} |\psi_1\rangle' \\ |\psi_2\rangle' \end{pmatrix}, \quad (2.6)$$

where “*” abbreviates the part which is not needed for our purpose, and

$$\begin{pmatrix} |\psi_1\rangle' \\ |\psi_2\rangle' \end{pmatrix} = \mathcal{U}^\dagger \begin{pmatrix} |\psi_1\rangle \\ |\psi_2\rangle \end{pmatrix}. \quad (2.7)$$

$|\psi_1\rangle'$ completely decouples from $|\psi_2\rangle'$, so that we can concentrate only on the equation for H_{eff} and $|\psi_1\rangle'$ in the subspace selected by η :

$$H_{\text{eff}}|\psi_1\rangle' = E|\psi_1\rangle'. \quad (2.8)$$

We set an ansatz for the similarity (unitary) transformation operator

$$\mathcal{U} = \begin{pmatrix} \mathcal{U}_{11} & \mathcal{U}_{12} \\ \mathcal{U}_{21} & \mathcal{U}_{22} \end{pmatrix} = \begin{pmatrix} (1 + A^\dagger A)^{-1/2} & -A^\dagger(1 + AA^\dagger)^{-1/2} \\ A(1 + A^\dagger A)^{-1/2} & (1 + AA^\dagger)^{-1/2} \end{pmatrix}. \quad (2.9)$$

It is convenient to use J

$$J = \begin{pmatrix} 1 & 0 \\ A & 1 \end{pmatrix}, \quad (2.10)$$

instead of A . In order for the off-diagonal parts in Eq. (2.6) to become zero, J must satisfy

$$(1 - \eta)(H'J + [H_0, J] - J\langle H'J \rangle)\eta = 0, \quad (2.11)$$

where we have introduced the notation $\langle \rangle$ as

$$\langle O \rangle \equiv \eta O \eta + (1 - \eta)O(1 - \eta) = \begin{pmatrix} O_{11} & 0 \\ 0 & O_{22} \end{pmatrix}. \quad (2.12)$$

Using Eqs. (2.6), (2.9), and (2.11), we formally obtain the effective Hamiltonian

$$H_{\text{eff}} = \eta \langle J^\dagger J \rangle^{-1/2} \langle J^\dagger H J \rangle \langle J^\dagger J \rangle^{-1/2} \eta, \quad (2.13)$$

but J is unknown so far.

In the interaction picture, Eq. (2.11) may be regarded as a differential equation

$$(1 - \eta) i \frac{dJ(t)}{dt} \eta = (1 - \eta) [H'(t)J(t) - J(t)\langle H'(t)J(t) \rangle] \eta, \quad (2.14)$$

where $J(0)$ is identified with J . $H'(t)$ and $J(t)$ are defined in this picture as

$$H'(t) \equiv e^{iH_0 t} H' e^{-iH_0 t} e^{\epsilon t}, \quad J(t) \equiv e^{iH_0 t} J e^{-iH_0 t} e^{\epsilon t}, \quad (2.15)$$

where $e^{\epsilon t}$ is an adiabatic factor with $\epsilon \rightarrow 0+$. We hereafter omit it in order to keep equations simple. Provided that we set the initial condition

$$J(-\infty) = 1, \quad (2.16)$$

J can be found order by order. Alternatively, if we solve

$$i \frac{dV(t)}{dt} = H'(t)V(t) - V(t)\langle H'(t)V(t) \rangle, \quad (2.17)$$

under the initial condition

$$V(-\infty) = 1, \quad (2.18)$$

J is given by

$$J = 1 + (1 - \eta)V(0)\eta = \begin{pmatrix} 1 & 0 \\ V_{21}(0) & 1 \end{pmatrix}. \quad (2.19)$$

It is easily found that the solution of Eq. (2.17) is given by

$$\begin{aligned} V(t) &= U(t)\langle U(t) \rangle^{-1} \\ &= \begin{pmatrix} U_{11}(t) & U_{12}(t) \\ U_{21}(t) & U_{22}(t) \end{pmatrix} \begin{pmatrix} U_{11}^{-1}(t) & 0 \\ 0 & U_{22}^{-1}(t) \end{pmatrix} \\ &= \begin{pmatrix} 1 & U_{12}(t)U_{22}^{-1}(t) \\ U_{21}(t)U_{11}^{-1}(t) & 1 \end{pmatrix}, \end{aligned} \quad (2.20)$$

where $U(t)$ is the usual time evolution operator

$$U(t) = \text{T exp} \left\{ -i \int_{-\infty}^t dt' H'(t') \right\}. \quad (2.21)$$

$U_{11}^{-1}(t)$ and $U_{22}^{-1}(t)$ are the inverse operators of $U_{11}(t)$ and $U_{22}(t)$ respectively. J is explicitly obtained from Eqs. (2.19) and (2.20), and then we expand it in the order of H' to obtain the effective Hamiltonian perturbatively:

$$J = \begin{pmatrix} 1 & 0 \\ U_{21}(t)U_{11}^{-1}(t) & 1 \end{pmatrix} = 1 + \sum_{n=1}^{\infty} J_n, \quad (2.22)$$

where n is the order of H' . The resultant effective Hamiltonian becomes

$$\begin{aligned} H_{\text{eff}} &= \frac{1}{2}\eta \left(H_0 + H' + H'J_1 + H'J_2 \right. \\ &\quad \left. + H'J_3 + \frac{1}{4}[J_1^\dagger J_1, H'J_1] \right) \eta + \text{h.c.} + \mathcal{O}(H'^5), \end{aligned} \quad (2.23)$$

to the fourth order. It is known that this can produce the TMO potential in the symmetrical pseudoscalar pion theory with the pseudovector coupling, which explains the properties of the deuteron very well.

Although Eq. (2.23) is general and it is very straightforward to calculate it, the calculation is absurdly tedious because J is not a time-ordered operator but a product of ones, and has particle-number-changing interactions. In order to renormalize the theory perturbatively, we need to calculate the counterterms but it is not manifest what sort of the divergences emerge in the effective Hamiltonian before doing actual calculations. It is not obvious either whether it is renormalizable or not even in the renormalizable theory.

§3. Construction and renormalization of the effective Hamiltonian

In this section, we give the construction method of the FSTO's effective Hamiltonian from Feynman diagrams and discuss the renormalization of it. First, we introduce the auxiliary operators F and G for convenience, and then show that the effective Hamiltonian is written in terms of them. G can be constructed from the same Feynman diagrams as those for S-matrix elements in the covariant perturbation theory. We give the rules for the construction of it and show that it is renormalized by the usual renormalization procedure. Lastly, we show that the effective Hamiltonian has the divergent terms even if G is renormalized. We discuss their role in diagonalizing the effective Hamiltonian.

3.1. Definitions of F and G

Let us define an operator

$$F \equiv \eta H' J \eta, \quad (3.1)$$

motivated by the first few terms in Eq. (2.23). We will show that the effective Hamiltonian can be rewritten in terms of H_0 and F . By using Eqs. (2.19) and (2.20), we write J as

$$J = \begin{pmatrix} 0 & 0 \\ 0 & 1 \end{pmatrix} + \begin{pmatrix} 1 & 0 \\ U_{21}(0)U_{11}^{-1}(0) & 0 \end{pmatrix} = (1 - \eta) + U(0)\eta\langle U(0) \rangle^{-1}\eta. \quad (3.2)$$

Therefore, F becomes

$$\begin{aligned} F &= \eta H' U(0) \eta \langle U(0) \rangle^{-1} \eta \\ &= G \eta \langle U(0) \rangle^{-1} \eta, \end{aligned} \quad (3.3)$$

where we define another operator G as

$$\begin{aligned} G &\equiv \eta H' U(0) \eta \\ &= \eta T \left\{ H'(0) \exp \left[-i \int_{-\infty}^0 dt H'(t) \right] \right\} \eta \\ &= \eta \left\{ H'(0) \right. \\ &\quad \left. + \sum_{n=1}^{\infty} (-i)^n \int_{-\infty}^0 dt_1 \int_{-\infty}^{t_1} dt_2 \cdots \int_{-\infty}^{t_{n-1}} dt_n H'(0) H'(t_1) H'(t_2) \cdots H'(t_n) \right\} \eta. \end{aligned} \quad (3.4)$$

As we will shortly see, to introduce G is crucial for using the the diagrammatic rules. An advantage for using G is that it is diagonal in the particle number space so that we can normal-order the products of G 's more easily than those of J 's and H' . Note that G is similar to the S-matrix operator but there is one important difference: the upper limit of the time integration is 0.

We can find that $\eta\langle U(t)\rangle\eta$ is written in terms of G , by integrating t' from $-\infty$ to t after sandwiching G between $e^{iH_0t'}$ and $e^{-iH_0t'}$:

$$\begin{aligned}
& -i \int_{-\infty}^t dt' G(t') \\
&= -i \int_{-\infty}^t dt' \eta \left\{ H'(t') \right. \\
&\quad \left. + \sum_{n=1}^{\infty} (-i)^{n+1} \int_{-\infty}^0 dt_1 \int_{-\infty}^{t_1} dt_2 \cdots \int_{-\infty}^{t_{n-1}} dt_n H'(t') H'(t_1 + t') H'(t_2 + t') \cdots H'(t_n + t') \right\} \eta \\
&= \eta \left\{ -i \int_{-\infty}^t dt' H'(t') \right. \\
&\quad \left. + \sum_{n=1}^{\infty} (-i)^{n+1} \int_{-\infty}^t dt' \int_{-\infty}^{t'} dt'_1 \int_{-\infty}^{t'_1} dt'_2 \cdots \int_{-\infty}^{t'_{n-1}} dt'_n H'(t') H'(t'_1) H'(t'_2) \cdots H'(t'_n) \right\} \eta \\
&= \eta\langle U(t)\rangle\eta - \eta, \tag{3.5}
\end{aligned}$$

where

$$G(t) = e^{iH_0t} G e^{-iH_0t}. \tag{3.6}$$

By substituting $\langle U(0)\rangle$ in Eq. (3.5) to Eq. (3.3), we can write F as

$$\begin{aligned}
F &= G \left[\eta - i \int_{-\infty}^0 dt G(t) \right]^{-1} \\
&= G \left\{ \eta + \sum_{n=1}^{\infty} \left[i \int_{-\infty}^0 dt G(t) \right]^n \right\}. \tag{3.7}
\end{aligned}$$

It is important that F depends only on G . Here, we expand F and G in the order of H' :

$$F = \sum_{m=1}^{\infty} F_m, \quad G = \sum_{m=1}^{\infty} G_m. \tag{3.8}$$

It is convenient to define

$$\mathcal{F}_n = \sum_{m=1}^n F_m, \quad \mathcal{G}_n = \sum_{m=1}^n G_m. \tag{3.9}$$

Also, we solve the differential equation

$$\begin{aligned}
i \frac{d}{dt} (J_1(t)^\dagger J_1(t)) &= -\eta H'(t) J_1(t) + J_1(t)^\dagger H'(t) \eta \\
&= -\eta \{ H'(t) + H'(t) J_1(t) \} \eta + \eta \{ H'(t) + J_1(t)^\dagger H'(t) \} \eta \\
&= -\mathcal{F}_2(t) + \mathcal{F}_2(t)^\dagger, \tag{3.10}
\end{aligned}$$

which is obtained from Eq. (2.14). It is easily found that

$$J_1^\dagger J_1 = i \int_{-\infty}^0 dt \{ \mathcal{F}_2(t) - \mathcal{F}_2^\dagger(t) \}, \tag{3.11}$$

under the initial condition $J_1(-\infty) = 0$. From Eqs. (3.1), (3.9) and (3.11), the term $\eta([J_1^\dagger J_1, H' J_1] + \text{h.c.})\eta$ in H_{eff} reads

$$\begin{aligned} & [J_1^\dagger J_1, \eta H' J_1] + \text{h.c.} \\ &= [J_1^\dagger J_1, \eta H' \eta + \eta H' J_1] + [\eta H' \eta + J_1^\dagger H' \eta, J_1^\dagger J_1] \\ &= i \int_{-\infty}^0 dt [\mathcal{F}_2(t) - \mathcal{F}_2^\dagger(t), \mathcal{F}_2] + \text{h.c.} \end{aligned} \quad (3.12)$$

Now we are ready to rewrite the effective Hamiltonian in terms of H_0 and F . We finally obtain the effective Hamiltonian in the useful form from Eqs. (2.23), (3.1), (3.9) and (3.12):

$$H_{\text{eff}} = \frac{1}{2}\eta \left\{ H_0 + \mathcal{F}_4 + \frac{i}{4} \int_{-\infty}^0 dt [\mathcal{F}_2(t) - \mathcal{F}_2^\dagger(t), \mathcal{F}_2] \right\} \eta + \text{h.c.} + \mathcal{O}(H'^5). \quad (3.13)$$

All interactions are written in terms of \mathcal{G}_n through \mathcal{F}_n to the fourth order in H' . To summarize, the effective Hamiltonian can be easily constructed once \mathcal{G}_n is obtained.

3.2. Rules for the construction of G

In this subsection, we give the rules for the construction of G from Feynman diagrams. We do not need to use the old fashioned perturbation theory. The knowledge in the covariant perturbation theory helps us to find them.

From Eq. (3.5), we immediately find that

$$\eta S \eta = \eta U(\infty) \eta = \eta - i \int_{-\infty}^{\infty} dt G(t), \quad (3.14)$$

where S is the familiar S-matrix operator. Comparing order by order, one can relate the n th order term of S to G_n as

$$\eta S_n \eta = -i \int_{-\infty}^{\infty} dt G_n(t). \quad (3.15)$$

It is important to make the difference between $\eta S_n \eta$ and G_n clearer. It is useful to rewrite them in terms of T-product and compare them in order to find the correspondence with Feynman diagrams:

$$\eta S_n \eta = \frac{(-i)^n}{n!} \int_{-\infty}^{\infty} dt_1 \int_{-\infty}^{\infty} dt_2 \cdots \int_{-\infty}^{\infty} dt_n \eta \text{T}(H'(t_1) H'(t_2) \cdots H'(t_n)) \eta, \quad (3.16)$$

$$G_n = \frac{(-i)^{n-1}}{(n-1)!} \int_{-\infty}^0 dt_1 \int_{-\infty}^0 dt_2 \cdots \int_{-\infty}^0 dt_{n-1} \eta \text{T}(H'(0) H'(t_1) H'(t_2) \cdots H'(t_{n-1})) \eta. \quad (3.17)$$

Wick's theorem tells us that T-products of $H'(t)$'s can be written as sums of normal-ordered products of creation and annihilation operators with the coefficients being amplitudes, which are given by the same Feynman diagrams. The difference between those arises from the time integrations. It is apparent that the role of $\int_{-\infty}^{\infty} dt$ is to give the energy conserving delta

function $2\pi\delta(E_{out} - E_{in})$ to each vertex in the Feynman diagrams, where E_{out} is an outgoing energy from the vertex and E_{in} is an incoming energy to it. Because the time integrations end at 0 in G_n , the energy denominators $(-i)(E_{out} - E_{in} - i\epsilon)^{-1}$ appear instead of the delta functions. The sign of an infinitesimal constant ϵ must be taken positive to ensure the convergence of the integrations at $t = -\infty$. n $H'(t)$'s become equivalent and cancel the factor $1/n!$ in S_n due to n time integrations, while there are $(n - 1)$ time integrations and the factor $1/(n - 1)!$ is canceled in G_n . But there is a $H'(0)$ which is not integrated, therefore there are n terms for each vertex which have $(n - 1)$ products of the energy denominators.

Let us consider the LF Yukawa model* as a concrete example. In this model, the interaction part of the Hamiltonian has the form of

$$H' = gH'^{(1)} + g^2H'^{(2)}. \quad (3.18)$$

The effect of $H'^{(2)}$ which is the instantaneous interaction is absorbed into the fermion propagator, and we hereafter omit it because we assume that LF diagrams are equivalent to the covariant one.** We define η as the projection operator for the two-body state which consists of a fermion and an anti-fermion. Because the power of g is equal to the number of the scalar fields and $\eta : (\text{odd } \phi\text{'s}) : \eta = 0$ is satisfied, a product of H' 's satisfy

$$\eta[H'(x_1^+)H'(x_2^+)\cdots H'(x_n^+)]^{(m)}\eta = 0, \quad (3.19)$$

for odd m , where the number in the brackets in the superscript means the order of g and $x^+ = (x^0 + x^3)/\sqrt{2}$ is LF time. \mathcal{F}_2 and \mathcal{F}_4 become

$$\mathcal{F}_2 = \mathcal{G}_2 + \mathcal{O}(g^4), \quad (3.20)$$

$$\mathcal{F}_4 = \mathcal{G}_4 + i\mathcal{G}_2 \int_{-\infty}^0 dx^+ \mathcal{G}_2(x^+) + \mathcal{O}(g^6). \quad (3.21)$$

G_n is written as

$$\begin{aligned} G_n = & \sum_{\lambda} \int_{p_1} \int_{p_2} \mathcal{M}_n \eta b_{\lambda}^{\dagger}(p_1) b_{\lambda}(p_2) \eta (2\pi)^3 \delta^3(p_1 - p_2) \\ & - \sum_{\lambda} \int_{p_1} \int_{p_2} \bar{\mathcal{M}}_n \eta d_{\lambda}^{\dagger}(p_1) d_{\lambda}(p_2) \eta (2\pi)^3 \delta^3(p_1 - p_2) \\ & - \sum_{\lambda_1} \sum_{\lambda_2} \sum_{\sigma_1} \sum_{\sigma_2} \int_{p_1} \int_{p_2} \int_{l_1} \int_{l_2} \mathcal{V}_n \\ & \times \eta b_{\lambda_1}^{\dagger}(p_1) d_{\sigma_1}^{\dagger}(l_1) d_{\sigma_2}(l_2) b_{\lambda_2}(p_2) \eta (2\pi)^3 \delta^3(p_1 + l_1 - p_2 - l_2), \end{aligned} \quad (3.22)$$

* Lagrangian and Hamiltonian in this model are given in Appendix A.

** It is explained at the last paragraph in Appendix A.

where we define

$$\int_p \equiv \int \frac{dp^+ d^2 p_\perp}{2p^+ (2\pi)^3} \theta(p^+), \quad (3.23)$$

$$\delta^3(p - q) \equiv \delta(p^+ - q^+) \delta^2(p_\perp - q_\perp). \quad (3.24)$$

We hereafter call p^- “energy” and (p^+, p_\perp) “three-momentum”. The creation and annihilation operators of the fermion, $b_\lambda^\dagger(p)$ and $b_\lambda(p)$, and ones of the anti-fermion, $d_\lambda^\dagger(p)$ and $d_\lambda(p)$, satisfy the anti-commutation relations

$$\{b_{\lambda_1}(p_1), b_{\lambda_2}^\dagger(p_2)\} = \{d_{\lambda_1}(p_1), d_{\lambda_2}^\dagger(p_2)\} = 2p_1^+ (2\pi)^3 \delta^3(p_1 - p_2) \delta_{\lambda_1 \lambda_2}, \quad (3.25)$$

and the other anti-commutators vanish. The minus signs which are attached to the second and third term of the right-hand side of Eq. (3.22) come from the normal-ordered products of the anti-fermion operators, but are just the convention. \mathcal{M}_n and $\bar{\mathcal{M}}_n$ correspond to the amplitude for the fermionic and anti-fermionic one-particle state respectively, and we have allowed for the conservation of the helicity. As we discuss in Sec. 3.3.1, these vanish under the physical (on-shell) renormalization condition.

\mathcal{V}_n is a potential between a fermion and an anti-fermion in G_n and is constructed by the n th order Feynman diagrams which have an incoming fermion and anti-fermion and outgoing ones. Since pair creations and annihilations of particles from the vacuum are forbidden due to the merit of the LF field theory, we must not include the disconnected diagrams.

There are three differences between our construction rules of \mathcal{V}_n and the usual Feynman rules for the general amplitudes:

- Assign a factor

$$-g\gamma_5 \frac{-i}{p_{out}^- - p_{in}^- - i\epsilon}, \quad (3.26)$$

to each vertex, where p_{out}^μ (p_{in}^μ) is the outgoing (incoming) four-momentum from (to) the vertex. The energy denominator corresponds to the energy conserving delta function in the Feynman rules.

- Assign an independent energy p^- for each propagator and integrate it. We do not impose the conservation of the energies.
- Attach a total energy difference $-(p_1^- + l_1^- - p_2^- - l_2^-)$ as an overall factor.

It is obvious that the first two differences come from the domain of the time integrations. The origin of the last one is that there are n terms which have different products of the energy denominators as mentioned above. For example, in the case of the diagram Fig. 1(a) we consider the energy denominators obtained from Eq. (3.17) with factors of i :

$$(-i)^3 i^4 \left[\left(\frac{-i}{l_1^- + k_2^- - q_1^- - i\epsilon} \right) \left(\frac{-i}{q_2^- - k_2^- - l_2^- - i\epsilon} \right) \left(\frac{-i}{k_1^- - q_2^- - p_2^- - i\epsilon} \right) \right]$$

$$\begin{aligned}
& + \left(\frac{-i}{p_1^- + q_1^- - k_1^- - i\epsilon} \right) \left(\frac{-i}{q_2^- - k_2^- - l_2^- - i\epsilon} \right) \left(\frac{-i}{k_1^- - q_2^- - p_2^- - i\epsilon} \right) \\
& + \left(\frac{-i}{p_1^- + q_1^- - k_1^- - i\epsilon} \right) \left(\frac{-i}{l_1^- + k_2^- - q_1^- - i\epsilon} \right) \left(\frac{-i}{k_1^- - q_2^- - p_2^- - i\epsilon} \right) \\
& + \left(\frac{-i}{p_1^- + q_1^- - k_1^- - i\epsilon} \right) \left(\frac{-i}{l_1^- + k_2^- - q_1^- - i\epsilon} \right) \left(\frac{-i}{q_2^- - k_2^- - l_2^- - i\epsilon} \right) \Big]. \quad (3.27)
\end{aligned}$$

The factor $(-i)^3$ comes from three time integrations $(-i \int_{-\infty}^0 dx^+)$, while the factor i^4 comes from four vertices $(-ig\bar{\psi}\gamma_5\phi\psi)$. In general, the total factor of i is $(-i)^{V-1}i^V$ where V is the number of vertices in the diagram. Since the sum is the combination of removing one from four denominators, we can make it a product of all the energy denominators:

$$\begin{aligned}
& = -(p_1^- + l_1^- - p_2^- - l_2^-) \left(\frac{-i}{p_1^- + q_1^- - k_1^- - i\epsilon} \right) \left(\frac{-i}{l_1^- + k_2^- - q_1^- - i\epsilon} \right) \\
& \quad \times \left(\frac{-i}{q_2^- - k_2^- - l_2^- - i\epsilon} \right) \left(\frac{-i}{k_1^- - q_2^- - p_2^- - i\epsilon} \right). \quad (3.28)
\end{aligned}$$

This factor corresponds to the elimination of the total energy conserving delta function.

Finally, \mathcal{V}_n becomes

$$\begin{aligned}
\mathcal{V}_n & = -(p_1^- + l_1^- - p_2^- - l_2^-) \sum_{\text{diagrams}} \int_{-\infty}^{\infty} \frac{dk_1^-}{2\pi} \int_{-\infty}^{\infty} \frac{dk_2^-}{2\pi} \cdots \int_{-\infty}^{\infty} \frac{dq_1^-}{2\pi} \int_{-\infty}^{\infty} \frac{dq_2^-}{2\pi} \cdots \\
& \quad \times \left(\frac{-i}{p_1^- - k_1^- - q_1^- - i\epsilon} \right) \left(\frac{-i}{l_1^- - k_2^- + q_2^- - i\epsilon} \right) \cdots \\
& \quad \times (-i\mathcal{A}_n), \quad (3.29)
\end{aligned}$$

where \mathcal{A}_n is the usual amplitude constructed from the Feynman diagrams but each energy of the propagators is an independent variable which is integrated outside of \mathcal{A}_n . Therefore, \mathcal{A}_n is constructed from the propagators $S_F(k)$ and $\Delta_F(q)$ with each independent energy, and the vertex $-g\gamma_5$, and the external fermion line $\bar{u}(p_1, \lambda_1)$, $u(p_2, \lambda_2)$, $v(l_1, \sigma_1)$, $\bar{v}(l_2, \sigma_2)$, and an integration of four-momentum for each loop. The three-momenta are conserved but energies are not.

Although each propagator includes both the loop and independent energy, it is easy to split them. For example, in the box diagram Fig. 1(a) the corresponding energy denominators are

$$\begin{aligned}
& \left(\frac{-i}{p_1^- + q_1^- - k_1^- - i\epsilon} \right), \left(\frac{-i}{l_1^- + k_2^- - q_1^- - i\epsilon} \right), \left(\frac{-i}{q_2^- - k_2^- - l_2^- - i\epsilon} \right), \\
& \text{and } \left(\frac{-i}{k_1^- - q_2^- - p_2^- - i\epsilon} \right). \quad (3.30)
\end{aligned}$$

If we consider q_2 as the loop momentum, by shifting momentum as

$$k_1 \rightarrow k_1 + q_2, \quad q_1 \rightarrow q_1 + q_2 \quad \text{and} \quad k_2 \rightarrow k_2 + q_2, \quad (3.31)$$

the denominators become

$$\left(\frac{-i}{p_1^- + q_1^- - k_1^- - i\epsilon} \right), \quad \left(\frac{-i}{l_1^- + k_2^- - q_1^- - i\epsilon} \right), \quad \left(\frac{-i}{-k_2^- - l_2^- - i\epsilon} \right),$$

and $\left(\frac{-i}{k_1^- - p_2^- - i\epsilon} \right),$ (3.32)

whose energies are assigned in Fig. 1(b). Because the loop momenta are not restricted by the usual conservation law of four-momenta in the covariant perturbation theory, it is apparent that the energy denominators do not depend on them.

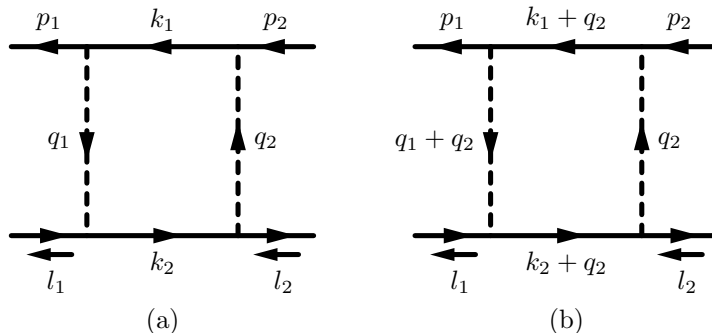


Fig. 1. An example of the one-loop box diagrams. In (a), energies are assigned to each propagator individually. In (b), energies are assigned to each propagator but the loop four-momentum q_2 is specified. All the three-momenta are conserved in both case. A continuous line corresponds to a fermion one, and a broken line correspond to a scalar one.

3.3. Renormalization of G

As mentioned in Sec. 3.2, \mathcal{A}_n corresponds to the usual amplitude. What is different from the amplitude is that energies of the propagators in \mathcal{A}_n are independent each other.

Even if the energies are not conserved, we can renormalize \mathcal{A}_n by the usual prescription in the covariant perturbation theory because UV divergences from the integrations of the loop momenta are local. They emerge as the coefficients of the polynomial of the other momenta. If the zeroth order term in those expansions includes a divergence, it is renormalized by shifting masses or a coupling constant. The other divergences are logarithmic and depend on momenta, then they must be renormalized by the field renormalization.

After renormalizing \mathcal{A}_n , we must consider the energy integrations. First, we show that the new divergence arises when we integrate the energies of the renormalized \mathcal{A}_n with the

energy denominators. In Hamiltonian formalism, it is not so trivial where the field renormalization constants come from because the energies are not conserved. We discuss the field renormalization and show that an ambiguity which may cancel the above divergence comes from the energy integrations.

3.3.1. Divergences in G

Even if \mathcal{A}_n is renormalized, new divergences may arise from the energy integrations in \mathcal{V}_n .

This problem does not occur in the one-particle states which correspond to the diagrams like in Fig. 2. From the on-shell condition

$$p_1^2 = p_2^2 = m^2, \quad (3.33)$$

and the three-momentum conservation law

$$p_1^+ = p_2^+, \quad p_{1\perp} = p_{2\perp}, \quad (3.34)$$

for the fermion line, the one-particle states conserve the energies:

$$p_1^- = \frac{p_{1\perp}^2 + m^2}{2p_1^+} = \frac{p_{2\perp}^2 + m^2}{2p_2^+} = p_2^-. \quad (3.35)$$

The same conservation law is applied to the anti-fermion line. It is obvious from Eq. (3.14) that G multiplied by the total energy conserving delta function is S . Therefore the one-particle states of G are equivalent to those of S . If we renormalize the self-energy part under the physical renormalization condition, \mathcal{M}_n and $\bar{\mathcal{M}}_n$ in Eq. (3.22) vanish. An example of the order g^2 will be demonstrated in Appendix B.

In multi-particle states, even though the external lines satisfy the on-shell condition and the three-momentum conservation law, one can not say that the total energy is conserved. We will show that such divergences disappear even in the multi-particle states except for the case that the outgoing external fermion line has a self-energy part.

First, we consider the one-particle irreducible part $\Gamma(k'_1, k'_2, \dots)$ of the renormalized \mathcal{A}_n , where k'_1, k'_2, \dots are the four-momenta of the propagators except for the loop momentum, and satisfy the three-momentum conservation law. Since $\Gamma(k'_1, k'_2, \dots)$ is covariant, the analysis for large four-momentum $k_i'^{\mu}$'s, which is used in the operator product expansion, is valid when we investigate the asymptotic behavior for large $k_i'^-$'s.¹⁴⁾ Therefore, after considering that the loop momenta associated to $k_i'^{\mu}$'s are as large as $k_i'^{\mu}$'s, we regard $k_i'^-$'s as larger than

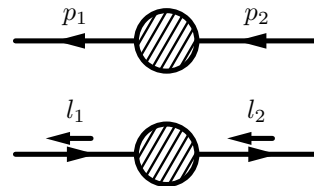


Fig. 2. A diagram of the one-particle state. The blob is a connected diagram.

k_i^+ 's and $k_{i\perp}$'s. By the power counting, the leading contribution comes from the self-energy part. For the scalar self-energy part, the leading behavior of $\Gamma(k'_1, k'_2, \dots)$ goes

$$\begin{aligned}\Gamma(k'_1, k'_2, \dots)_{\text{scalar self-energy}} &\sim \sum_{ij} c_{ij} k'_i \cdot k'_j \\ &\sim \sum_{ij} c_{ij} (k_i'^+ k_j'^- + k_i'^- k_j'^+),\end{aligned}\quad (3.36)$$

and for the fermion self-energy,

$$\begin{aligned}\Gamma(k'_1, k'_2, \dots)_{\text{fermion self-energy}} &\sim \sum_i c_i k'_i, \\ &\sim \sum_i c_i k_i'^- \gamma^+, \end{aligned}\quad (3.37)$$

where c_{ij} and c_i may depend on logarithmic factor of k_i' 's. It is important that both are proportional to $k_i'^-$'s at most. If we multiply $\Gamma(k'_1, k'_2, \dots)$ by the energy denominators and integrate over the energies, it seems that it behaves as logarithmically divergent. But such term must not exist when the energies are conserved, that is, such divergence is not possible in S , so it must be proportional to the total energy difference. For the scalar self-energy in the internal line, we regard the blob in Fig. 3(a) as $\Gamma(k'_1, k'_2, \dots)_{\text{scalar self-energy}}$. The contribution from it is

$$\begin{aligned}&\int_{-\infty}^{\infty} \frac{dk_1'^-}{2\pi} \int_{-\infty}^{\infty} \frac{dk_2'^-}{2\pi} \cdots \frac{-i}{q_2^- - k_1'^- - k_2'^- - i\epsilon} \cdots \Gamma(k'_1, k'_2, \dots)_{\text{scalar self-energy}} \\ &\sim \frac{-i}{q_2^- - q_1^- - i\epsilon} \{i\Pi(q_1, q_2) + iq^+(q_2^- - q_1^-) \log(q'^+ \Lambda^-) \\ &\quad + (q_2^- - q_1^-)(\text{finite terms})\},\end{aligned}\quad (3.38)$$

where $\Pi(q_1, q_2)$ becomes the usual scalar self-energy if we replace the energy denominator with the energy delta function, and Λ^- is the UV cutoff of the energy. The second and third term are proportional to $(q_2^- - q_1^-)$ by the above reason. q^+ and q'^+ are proper longitudinal momenta. The divergence only arises in the second term because Eq. (3.38) is regarded as Taylor expansion in $(q_2^- - q_1^-)$. The first term is the ordinary renormalized finite term. Although the second term is divergent, it is found that it behaves as logarithmically divergent at most by Lorentz covariance and the power counting. The third term converges because the second term is logarithmically divergent and a differentiation by the energy decreases the power of the divergence by one.

Although Eq. (3.38) includes the divergence, it vanishes when it is inserted in the internal scalar line. Let us consider scalar propagators and energy denominators in vertices around the blob in Fig. 3(a). It is crucial that the second term in Eq. (3.38) does not depend q_1^-

and q_2^- . The total contribution from the second term is

$$\begin{aligned}
& \int_{-\infty}^{\infty} \frac{dq_1^-}{2\pi} \int_{-\infty}^{\infty} \frac{dq_2^-}{2\pi} \frac{-i}{k_4^- - k_3^- - q_2^- - i\epsilon} \Delta_F(q_2) \\
& \times \left\{ \frac{-i}{q_2^- - q_1^- - i\epsilon} i q^+(q_2^- - q_1^-) \log(q^+ \Lambda^-) \right\} \Delta_F(q_1) \frac{-i}{q_1^- + k_2^- - k_1^- - i\epsilon} \\
& = \Delta_F(k_4 - k_3) \theta(-q_2^+) q^+ \log(q^+ \Lambda^-) \Delta_F(k_1 - k_2) \theta(q_1^+). \tag{3.39}
\end{aligned}$$

But the three-momenta are conserved ($q_1^+ = q_2^+$, $q_{1\perp} = q_{2\perp}$), so it is obvious that Eq. (3.39) vanishes.

The fermion self-energy is logarithmically divergent like Eq. (3.38). For the internal fermion line in Fig. 3(b), the contribution from the divergent part is

$$\begin{aligned}
& \int_{-\infty}^{\infty} \frac{dk_2^-}{2\pi} \int_{-\infty}^{\infty} \frac{dk_3^-}{2\pi} \frac{-i}{k_4^- + q_2^- - k_3^- - i\epsilon} S_F(k_3) \\
& \times \left\{ \frac{-i}{k_3^- - k_2^- - i\epsilon} i \gamma^+(k_3^- - k_2^-) \log(k^+ \Lambda^-) \right\} S_F(k_2) \frac{-i}{k_2^- - k_1^- - q_1^- - i\epsilon}, \tag{3.40}
\end{aligned}$$

where k^+ is a proper longitudinal momentum. Unlike $\Delta_F(q)$, $S_F(k)$ has a term which does not depend on the energy but is proportional to γ^+ :

$$S_F(k) = \frac{i\gamma^+}{2k^+} + i \frac{\frac{k_\perp^2 + m^2}{2k^+} \gamma^+ + k^+ \gamma^- - k_\perp \cdot \gamma_\perp + m}{k^2 - m^2 + i\epsilon}. \tag{3.41}$$

Fortunately, γ^+ has the property that $(\gamma^+)^2 = 0$, so the first term has no effect in Eq. (3.40). The second term is discussed in the same way as in the scalar case, and then Eq. (3.40) vanishes.

Note that the above mechanism only works for the internal lines. The diagrams which have the self-energy in the external fermion line may have the same divergence. We consider the incoming external fermion line like in Fig. 3(c). The contribution from the divergent part becomes

$$\begin{aligned}
& \int_{-\infty}^{\infty} \frac{dk_1^-}{2\pi} \frac{-i}{q_1^- + k_2^- - k_1^- - i\epsilon} S_F(k_1) \left\{ \frac{-i}{k_1^- - p_2^- - i\epsilon} i \gamma^+(k_1^- - p_2^-) \log(k^+ \Lambda^-) \right\} u(p_2, \lambda_2) \\
& = S_F(q_1 + k_2) \theta(-p_2^+) \log(k^+ \Lambda^-) u(p_2, \lambda_2), \tag{3.42}
\end{aligned}$$

where all the three-momenta are conserved. Since the incoming line has the positive longitudinal momentum $p_2^+ > 0$, this vanishes. In the case of the outgoing external fermion line like in Fig. 3(d), the contribution from the divergent part becomes

$$\begin{aligned}
& \int_{-\infty}^{\infty} \frac{dk_1^-}{2\pi} \bar{u}(p_1, \lambda_1) \left\{ \frac{-i}{p_1^- - k_1^- - i\epsilon} i \gamma^+(p_1^- - k_1^-) \log(k^+ \Lambda^-) \right\} S_F(k_1) \frac{-i}{k_1^- - k_2^- - q_1^- - i\epsilon} \\
& = \bar{u}(p_1, \lambda_1) S_F(k_2 + q_1) \theta(p_1^+) \log(k^+ \Lambda^-). \tag{3.43}
\end{aligned}$$

Since the outgoing line satisfies $p_1^+ > 0$, this does not vanish and is logarithmically divergent.

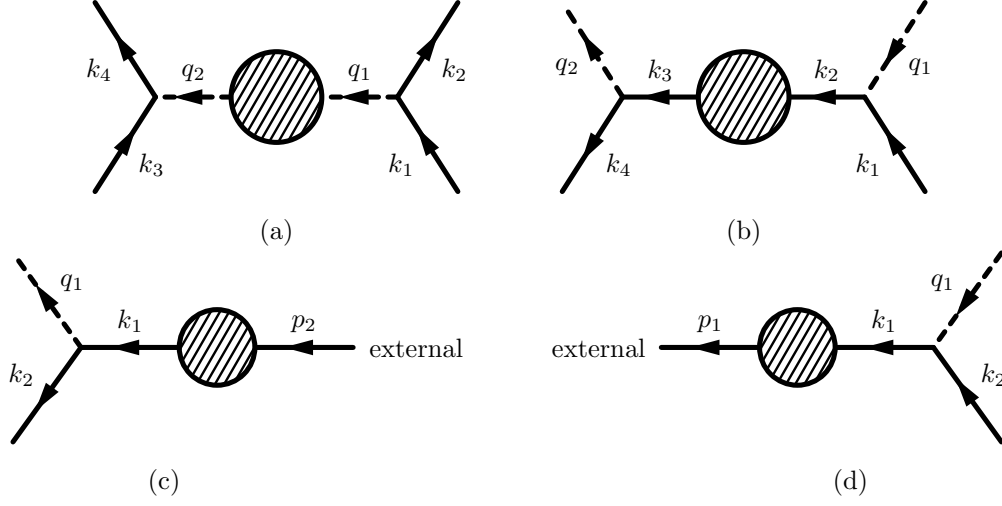


Fig. 3. (a) is a diagram which includes a scalar self-energy in an internal scalar line. (b), (c), and (d) are ones including a fermion self-energy part in an internal, incoming-external and outgoing-external fermion line, respectively. In all the case, the three-momenta are conserved. The blobs are some one-particle-irreducible graphs.

3.3.2. Field renormalization

The counterterms for the fields have the same behaviors as those in Eqs. (3.36) and (3.37). The energy integrations of those yield not logarithmic divergences but ambiguous constants.

First, let us consider the case of the scalar field. We define the field renormalization constant as Z_3 . The corresponding counterterm in our rules is

$$\text{Fig. 4(a)} = \int_{-\infty}^{\infty} \frac{dk^-}{2\pi} \frac{-i}{q_2^- - k^- - i\epsilon} (1 - Z_3) \Delta_F^{-1}(k) \frac{-i}{k^- - q_1^- - i\epsilon}, \quad (3.44)$$

where the three-momenta are conserved ($k_1^+ = q_1^+ = q_2^+$, $k_{1\perp} = q_{1\perp} = q_{2\perp}$) and we omit the scalar propagators attached on both sides of it. This is the usual field renormalization and cancels the logarithmic divergence which comes from the integration of the loop momentum. Carrying out the energy integration, we obtain

$$(1 - Z_3) \left[cq_1^+ + \frac{-i}{q_2^- - q_1^- - i\epsilon} \Delta_F^{-1}(q_1) \right], \quad (3.45)$$

where c is an ambiguous constant which depends on the way of taking the limit $k^- \rightarrow \pm\infty$. More generally, the contribution from n counterterms connected by the scalar propagators is

$$\text{Fig. 4(b)} = \int_{-\infty}^{\infty} \frac{dk_1^-}{2\pi} \int_{-\infty}^{\infty} \frac{dk_2^-}{2\pi} \cdots \int_{-\infty}^{\infty} \frac{dk_n^-}{2\pi} \int_{-\infty}^{\infty} \frac{dq_2^-}{2\pi} \int_{-\infty}^{\infty} \frac{dq_3^-}{2\pi} \cdots \int_{-\infty}^{\infty} \frac{dq_n^-}{2\pi}$$

$$\begin{aligned}
& \frac{-i}{q_{n+1}^- - k_n^- - i\epsilon} (1 - Z_3) \Delta_F^{-1}(k_n) \frac{-i}{k_n^- - q_n^- - i\epsilon} \cdots \\
& \cdots (1 - Z_3) \Delta_F^{-1}(k_2) \frac{-i}{k_2^- - q_2^- - i\epsilon} \Delta_F(q_2) \frac{-i}{q_2^- - k_1^- - i\epsilon} (1 - Z_3) \Delta_F^{-1}(k_1) \frac{-i}{k_1^- - q_1^- - i\epsilon} \\
& = (1 - Z_3)^n \left[s_n(q_1^+) q_1^+ + \frac{-i}{q_{n+1}^- - q_1^- - i\epsilon} \Delta_F^{-1}(q_1) \right], \tag{3.46}
\end{aligned}$$

where all the three-momenta are conserved. $s_n(q^+)$ is defined as

$$s_n(q^+) = a_n \theta(q^+) + b_n \theta(-q^+), \tag{3.47}$$

where a_n and b_n are ambiguous constants because there is an ambiguity of the order of the energy integrations.* If we insert it in an internal scalar line, the contribution becomes

$$\begin{aligned}
\text{Fig. 4(c)} &= \int_{-\infty}^{\infty} \frac{dq_1^-}{2\pi} \int_{-\infty}^{\infty} \frac{dq_{n+1}^-}{2\pi} \frac{-i}{k_4^- - k_3^- - q_{n+1}^- - i\epsilon} \Delta_F(q_{n+1}) \\
&\quad \times (1 - Z_3)^n \left[s_n(q_1^+) q_1^+ + \frac{-i}{q_{n+1}^- - q_1^- - i\epsilon} \Delta_F^{-1}(q_1) \right] \\
&\quad \times \Delta_F(q_1) \frac{-i}{q_1^- + k_2^- - k_1^- - i\epsilon} \\
&= \Delta_F(k_4 - k_3) \theta(-q_{n+1}^+) (1 - Z_3)^n s_n(q_1^+) q_1^+ \Delta_F(k_1 - k_2) \theta(q_1^+) \\
&\quad + \int_{-\infty}^{\infty} \frac{dq^-}{2\pi} \frac{-i}{k_4^- - k_3^- - q^- - i\epsilon} (1 - Z_3)^n \Delta_F(q) \frac{-i}{q^- + k_2^- - k_1^- - i\epsilon} \\
&= \int_{-\infty}^{\infty} \frac{dq^-}{2\pi} \frac{-i}{k_4^- - k_3^- - q^- - i\epsilon} (1 - Z_3)^n \Delta_F(q) \frac{-i}{q^- + k_2^- - k_1^- - i\epsilon}. \tag{3.48}
\end{aligned}$$

This does not depend on $s_n(q^+)$ and is equivalent to a free propagator multiplied by the constant $(1 - Z_3)^n$. The mechanism that $s_n(q^+)$ vanishes is the same as one that the logarithmic divergence in the self-energy does. We take the sum of the diagrams like in Fig. 4(d) and obtain the result

$$\begin{aligned}
& \left(1 + \sum_{n=1}^{\infty} (1 - Z_3)^n \right) \int_{-\infty}^{\infty} \frac{dq^-}{2\pi} \frac{-i}{k_4^- - k_3^- - q^- - i\epsilon} \Delta_F(q) \frac{-i}{q^- + k_2^- - k_1^- - i\epsilon} \\
&= \frac{1}{Z_3} \int_{-\infty}^{\infty} \frac{dq^-}{2\pi} \frac{-i}{k_4^- - k_3^- - q^- - i\epsilon} \Delta_F(q) \frac{-i}{q^- + k_2^- - k_1^- - i\epsilon}, \tag{3.49}
\end{aligned}$$

where the three-momenta are conserved. This property is the same as that of the usual field renormalization.

Similarly, we can discuss the fermion field. If we connect n counterterms for the fermion field with fermion propagators, the contribution becomes

$$\text{Fig. 5(a)} = \int_{-\infty}^{\infty} \frac{dq_1^-}{2\pi} \int_{-\infty}^{\infty} \frac{dq_2^-}{2\pi} \cdots \int_{-\infty}^{\infty} \frac{dq_n^-}{2\pi} \int_{-\infty}^{\infty} \frac{dk_2^-}{2\pi} \int_{-\infty}^{\infty} \frac{dk_3^-}{2\pi} \cdots \int_{-\infty}^{\infty} \frac{dk_n^-}{2\pi}$$

* See Appendix C.

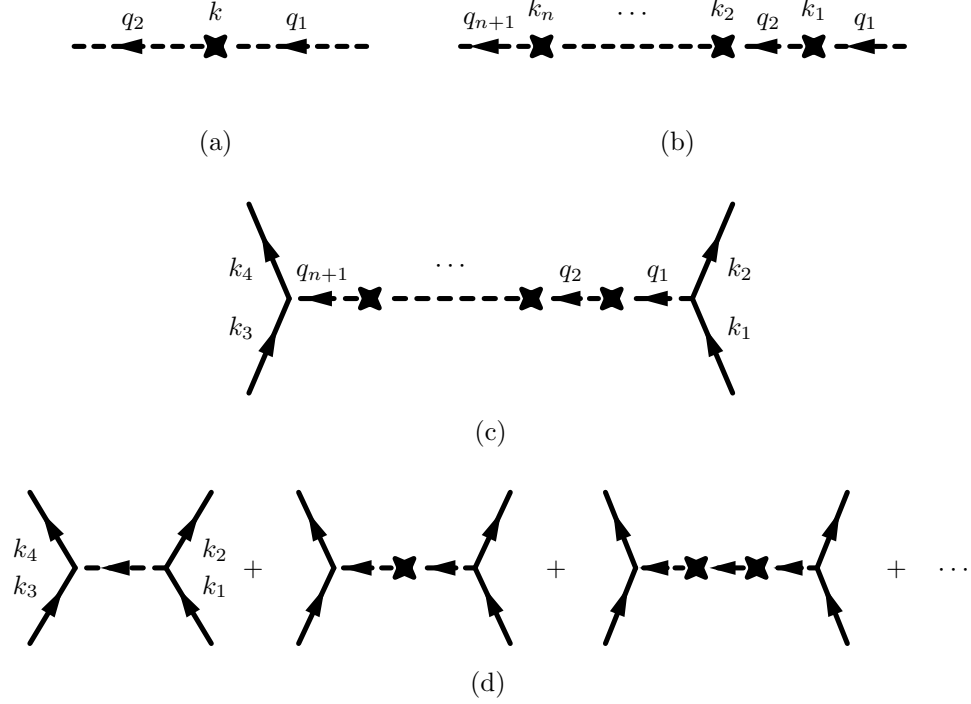


Fig. 4. Diagrams which contribute to the renormalization of the scalar field. X means a counterterm for the scalar field. (a) is a diagram which have a counterterm for the scalar field between scalar lines. q_1 and q_2 are four-momenta assigned to the external scalar lines and k is one for the counterterm. (b) is a diagram which have n counterterms connected by the scalar propagators. In (c), (b) is inserted between two vertices. (d) is an infinite sum of the diagrams (c). In all the case, the three-momenta are conserved.

$$\begin{aligned}
& \frac{-i}{k_{n+1}^- - q_n^- - i\epsilon} (1 - Z_2) S_F^{-1}(q_n) \frac{-i}{q_n^- - k_n^- - i\epsilon} \cdots \\
& \cdots (1 - Z_2) S_F^{-1}(q_2) \frac{-i}{q_2^- - k_2^- - i\epsilon} S_F(k_2) \frac{-i}{k_2^- - q_1^- - i\epsilon} (1 - Z_2) S_F^{-1}(q_1) \frac{-i}{q_1^- - k_1^- - i\epsilon} \\
& = (1 - Z_2)^n \left[f_n(k_1^+) \gamma^+ + \frac{-i}{k_{n+1}^- - k_1^- - i\epsilon} S_F^{-1}(k_1) \right], \tag{3-50}
\end{aligned}$$

where all the three-momenta are conserved and Z_2 is the field renormalization constant for the fermion field. The function $f_n(k^+)$ is defined as

$$f_n(k^+) = c_n \theta(k^+) + d_n \theta(-k^+), \tag{3-51}$$

where c_n and d_n are ambiguous constants due to a similar ambiguity.

When we insert Fig. 5(a) into the internal fermion line, the contribution from it is given by

$$\text{Fig. 5(b)} = \int_{-\infty}^{\infty} \frac{dk_1^-}{2\pi} \int_{-\infty}^{\infty} \frac{dk_{n+1}^-}{2\pi} \frac{-i}{q_2^- + p_2^- - k_{n+1}^- - i\epsilon} S_F(k_{n+1})$$

$$\begin{aligned}
& \times (1 - Z_2)^n \left[f_n(k_1^+) \gamma^+ + \frac{-i}{k_{n+1}^- - k_1^- - i\epsilon} S_F^{-1}(k_1) \right] \\
& \times S_F(k_1) \frac{-i}{k_1^- - q_1^- - p_1^- - i\epsilon} \\
& = S_F(q_2 + p_2) \theta(-k_{n+1}^+) (1 - Z_2)^n f_n(k_1^+) \gamma^+ S_F(q_1 + p_1) \theta(k_1^+) \\
& + \int_{-\infty}^{\infty} \frac{dk^-}{2\pi} \frac{-i}{q_2^- + p_2^- - k^- - i\epsilon} (1 - Z_2)^n S_F(k) \frac{-i}{k^- - q_1^- - p_1^- - i\epsilon} \\
& = \int_{-\infty}^{\infty} \frac{dk^-}{2\pi} \frac{-i}{q_2^- + p_2^- - k^- - i\epsilon} (1 - Z_2)^n S_F(k) \frac{-i}{k^- - q_1^- - p_1^- - i\epsilon}, \quad (3.52)
\end{aligned}$$

which is a free propagator multiplied by the constant $(1 - Z_2)^n$ and the energy denominators. An infinite sum of the diagrams becomes

$$\frac{1}{Z_2} \int_{-\infty}^{\infty} \frac{dk^-}{2\pi} \frac{-i}{q_2^- + p_2^- - k^- - i\epsilon} S_F(k) \frac{-i}{k^- - q_1^- - p_1^- - i\epsilon}. \quad (3.53)$$

As a result, $f_n(k^+)$ does not affect the fermion propagator.

For the incoming external fermion line, the contribution from the n connected counterterms is

$$\begin{aligned}
\text{Fig. 5(c)} & = (1 - Z_2)^n [f_n(k_1^+) \theta(-k_1^+) + 1] u(k_1, \lambda) \frac{-i}{q_1^- + p_1^- - k_1^- - i\epsilon} \\
& = (1 - Z_2)^n u(k_1, \lambda) \frac{-i}{q_1^- + p_1^- - k_1^- - i\epsilon}, \quad (3.54)
\end{aligned}$$

where $k_1^2 = m^2$ and $k_1^+ > 0$. Of course, all the three-momenta are conserved. In this case, $f_n(k^+)$ does not affect it. The infinite sum becomes

$$\frac{1}{Z_2} u(k, \lambda) \frac{-i}{q_1^- + p_1^- - k^- - i\epsilon}, \quad (3.55)$$

which is $1/Z_2$ times the tree external line. k^μ is the momentum of the external fermion.

For the outgoing external fermion line, the contribution is

$$\begin{aligned}
\text{Fig. 5(d)} & = (1 - Z_2)^n [f_n(k_{n+1}^+) \theta(k_{n+1}^+) + 1] \bar{u}(k_{n+1}, \lambda) \frac{-i}{k_{n+1}^- - q_1^- - p_1^- - i\epsilon} \\
& = (1 - Z_2)^n (c_n + 1) \bar{u}(k_{n+1}, \lambda) \frac{-i}{k_{n+1}^- - q_1^- - p_1^- - i\epsilon}, \quad (3.56)
\end{aligned}$$

where $k_{n+1}^2 = m^2$ and $k_{n+1}^+ > 0$. The infinite sum becomes

$$\left\{ 1 + \sum_{n=1}^{\infty} (1 - Z_2)^n (c_n + 1) \right\} \bar{u}(k, \lambda) \frac{-i}{k^- - q_1^- - p_1^- - i\epsilon}, \quad (3.57)$$

which is the tree external line multiplied by the constant. Note that c_n may not be equal to zero.

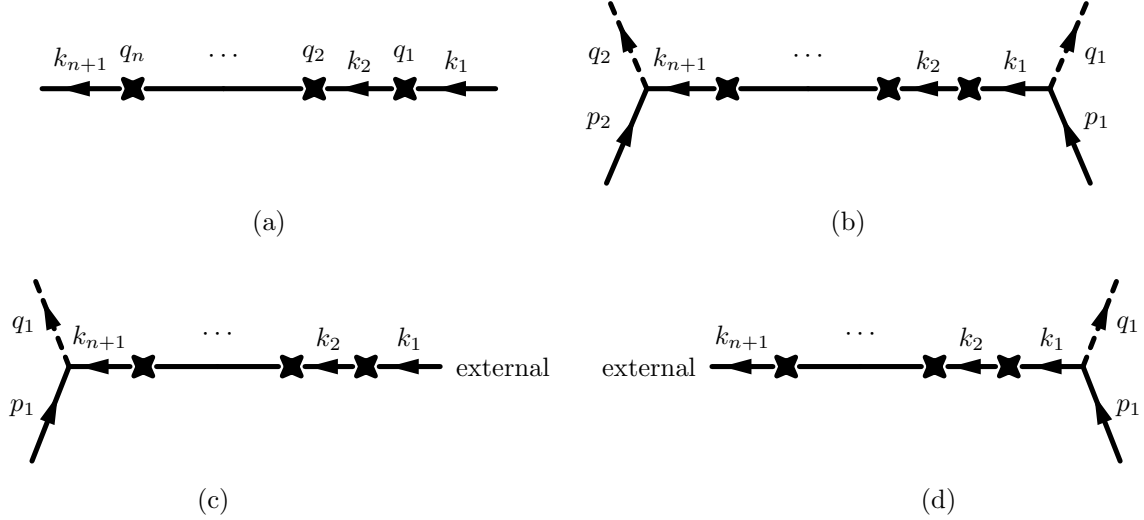


Fig. 5. Diagrams which contribute to the renormalization of the fermion field. X means a counterterm for the fermion field. (a) is a diagram which have n counterterms connected by the fermion propagators. In (b), (a) is inserted between two vertices. In (c), (a) is attached to the vertex and connected to the incoming line, and $k_1 = m^2$ and $k_1^+ > 0$ is satisfied. In (d), (a) is attached to the vertex and connected to the outgoing line, and $k_{n+1} = m^2$ and $k_{n+1}^+ > 0$ is satisfied. In all the case, the three-momenta are conserved.

3.3.3. Summary of the renormalization of G

We have shown that UV divergences from the loop integrations are renormalized by the usual procedure in the covariant perturbation theory. After renormalizing \mathcal{A}_n , we carry out the energy integrations. As a result, the new UV divergence and ambiguous constant c_n arise only from the diagrams that the fermion self-energy and its counterterm are inserted into the outgoing external line.

We fix c_n so that it can remove the above divergence. This is always possible because both live in the same place and are closely related. Although it is not the only way to fix c_n , we consider that it is natural for both to cancel each other.

3.4. Divergences in H_{eff}

In Sec. 3.3, we have shown that G is not divergent after renormalizing it by the usual prescription in the usual perturbation theory. In this subsection, we show that H_{eff} is divergent even if G is finite.

From Eqs. (3.13), (3.20), and (3.21), the effective Hamiltonian is written as

$$\begin{aligned}
 H_{\text{eff}} = & \frac{1}{2}\eta \left\{ H_0 + \mathcal{G}_4 + i\mathcal{G}_2 \int_{-\infty}^0 dx^+ \mathcal{G}_2(x^+) \right. \\
 & \left. + \frac{i}{4} \int_{-\infty}^0 dx^+ [\mathcal{G}_2(x^+) - \mathcal{G}_2^\dagger(x^+), \mathcal{G}_2] \right\} \eta + \text{h.c.} + \mathcal{O}(g^6), \quad (3.58)
 \end{aligned}$$

to the order of g^4 . We can renormalize \mathcal{G}_2 and \mathcal{G}_4 , but new divergences arise from the product of \mathcal{G}_2 . One of the examples is a product of two one-scalar-exchange diagrams in Fig. 6. The corresponding term in \mathcal{G}_2 is

$$\begin{aligned} \mathcal{G}_2^{\text{ex}} &= -i \sum_{\lambda_1} \sum_{\lambda_2} \sum_{\sigma_1} \sum_{\sigma_2} \int_{p_1} \int_{p_2} \int_{l_1} \int_{l_2} \bar{u}(p_1, \lambda_1) (-g\gamma_5) u(p_2, \lambda_2) \bar{v}(l_2, \sigma_2) (-g\gamma_5) v(l_1, \sigma_1) \\ &\quad \times [\Delta_F(l_2 - l_1) \theta(l_2^+ - l_1^+) + \Delta_F(p_1 - p_2) \theta(p_2^+ - p_1^+)] \\ &\quad \times \eta b_{\lambda_1}^\dagger(p_1) d_{\sigma_1}^\dagger(l_1) d_{\sigma_2}(l_2) b_{\lambda_2}(p_2) \eta (2\pi)^3 \delta^3(p_1 + l_1 - p_2 - l_2), \end{aligned} \quad (3.59)$$

where we have integrated the energy of $\Delta_F(q)$. The product of two $\mathcal{G}_2^{\text{ex}}$'s included in the third term of Eq. (3.58) is

$$\begin{aligned} &i\mathcal{G}_2^{\text{ex}} \int_{-\infty}^0 dx^+ \mathcal{G}_2^{\text{ex}}(x^+) \\ &= \frac{g^4}{16\pi^2} \log \Lambda_\perp^2 \sum_\lambda \sum_\sigma \int_{p_1} \int_{p_2} \int_{l_1} \int_{l_2} \sqrt{x(1-x)x'(1-x')} \\ &\quad \times \left\{ \frac{\theta(x-x')}{1-x'} \left(\log \frac{x}{x'} + \frac{1}{x} \right) + \frac{\theta(x'-x)}{x'} \left(\log \frac{1-x}{1-x'} + \frac{1}{1-x} \right) \right\} \\ &\quad \times \eta b_\lambda^\dagger(p_1) d_\sigma^\dagger(l_1) d_\sigma(l_2) b_\lambda(p_2) \eta (2\pi)^3 \delta^3(p_1 + l_1 - p_2 - l_2) + (\text{finite terms}), \end{aligned} \quad (3.60)$$

where Λ_\perp is the cutoff of the transverse momentum of the external fermion. x and x' are defined as

$$x = \frac{p_1^+}{p_1^+ + l_1^+}, \quad x' = \frac{p_2^+}{p_2^+ + l_2^+}, \quad (3.61)$$

respectively. Eq. (3.60) is logarithmically divergent as $\Lambda_\perp \rightarrow \infty$. A Feynman box diagram, which is finite by the power counting, consists of the sum of the various time-ordered diagrams which may be divergent individually. The above product is one of such and is logarithmically divergent.

It is important to recognize that H_{eff} should be divergent. The reason is understood by the perturbative diagonalization of it:

$$\begin{aligned} E_{\text{pert}} &= \frac{1}{2} \langle \alpha | \left\{ H_0 + \mathcal{G}_4 \right. \\ &\quad \left. + \frac{i}{2} \mathcal{G}_2 \int_{-\infty}^0 dx^+ \mathcal{G}_2(x^+) + \frac{i}{2} \int_{-\infty}^0 dx^+ \mathcal{G}_2(x^+) \mathcal{G}_2 + \text{h.c.} \right\} | \alpha \rangle + \mathcal{O}(g^6), \end{aligned} \quad (3.62)$$

where $|\alpha\rangle$ is an eigenstate of H_0 . Because the logarithmic divergence in Eq. (3.60) comes from the integral of the three-momentum of the intermediate state, the divergences of

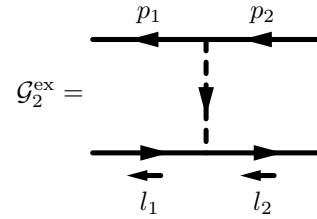


Fig. 6. The one-scalar-exchange diagram which contributes to \mathcal{G}_2 .

$\frac{i}{2} \int_{-\infty}^0 dx^+ \mathcal{G}_2(x^+) \mathcal{G}_2$ and of $\frac{i}{2} \mathcal{G}_2 \int_{-\infty}^0 dx^+ \mathcal{G}_2(x^+)$ have the opposite sign, and they cancel each other. In general, using the eigenstates of H_0 and its complete set, we obtain the matrix element

$$\begin{aligned}
& \langle \alpha | \left\{ \frac{i}{2} \mathcal{G}_2 \int_{-\infty}^0 dx^+ \mathcal{G}_2(x^+) + \frac{i}{2} \int_{-\infty}^0 dx^+ \mathcal{G}_2(x^+) \mathcal{G}_2 \right\} | \beta \rangle \\
&= \sum_{\gamma} \langle \alpha | \mathcal{G}_2 | \gamma \rangle \langle \gamma | \mathcal{G}_2 | \beta \rangle \frac{1}{2} \left(\frac{1}{p_{\gamma}^- - p_{\beta}^- - i\epsilon} + \frac{1}{p_{\alpha}^- - p_{\gamma}^- - i\epsilon} \right) \\
&= \sum_{\gamma} \langle \alpha | \mathcal{G}_2 | \gamma \rangle \langle \gamma | \mathcal{G}_2 | \beta \rangle \frac{1}{2} \frac{(p_{\alpha}^- - p_{\beta}^-)}{(p_{\gamma}^- - p_{\beta}^- - i\epsilon)(p_{\alpha}^- - p_{\gamma}^- - i\epsilon)}, \tag{3.63}
\end{aligned}$$

in which the power of the intermediate energy p_{γ}^- is decreased by one, and thus the power of the transverse momentum of the intermediate states by two.

It is important that although these divergences must be canceled by adding the artificial counterterms in the other similarity methods, they will *automatically* arise in the higher order terms in our method. As shown in Appendix B, if we diagonalize the effective Hamiltonian to the order of g^2 , the eigenvalue is divergent. In general, such divergences are mainly related to the box diagrams and arise not only in this case but also in the case of TD approximation in $(3+1)$ dimension.¹³⁾ Eq. (3.63) says that such divergences are canceled if we include g^4 order terms, then the divergences in the eigenvalue are weakened. However, new divergences arise in diagonalizing the effective Hamiltonian due to new interactions. We expect that they are canceled by the higher order interactions because the exact eigenvalue should not depend on the cutoff and the similarity transformation does not change the eigenvalue.

§4. Summary and discussions

In this paper, we have shown that the effective Hamiltonian, which is obtained by the FSTO's similarity transformation in the particle number space, can be written in terms only of G (or F) to the fourth order in H' .

To introduce G is crucial for constructing the effective Hamiltonian more easily than in the traditional way especially in the higher orders. G has a favorable property that it is diagonal in the particle number space. Since it also has the same form of the formula of the S-matrix operator, we can use the Feynman diagrams and the rules mentioned in Sec. 3.2 in the LF Yukawa model. By using the knowledge in the covariant perturbation theory, we can avoid the complexity in calculating it and make the renormalization procedure transparent. Note that our construction rules are a little bit different from the usual Feynman rules because energies are not conserved in each vertices.

The divergences due to the integrations of the loop momenta are renormalized by the familiar prescription in the covariant perturbation theory. The divergences due to the energy integrations can be canceled by terms which come from the ambiguity of the counterterms for the fields.

The mechanism of the cancellation of the extra divergences from the energy integrations is valid only in the LF field theory. It will be applied not only to the LF Yukawa model but also to the other LF models. Although we can not use it in the ET field theory, we expect that more precise integrations and treatment of the limit are necessary for the cancellation of the divergences.

Although G is constructed by Feynman diagrams and renormalized, the effective Hamiltonian has divergent terms which are written in terms of products of the renormalized those. It is very important that such terms do not need the counterterms but work as those which cancel the divergences in diagonalizing the effective Hamiltonian. Although the exact eigenvalue should not depend on the cutoff, our method is perturbative, so it is not possible to treat nonperturbative divergences in diagonalization and to get the exact eigenvalue. It is highly desired to find the nonperturbative counterterms for it. When we find the low energy states, our method is useful in small coupling region enough to allow one to ignore the cutoff dependence if the cutoff is much larger than lower eigenvalues.

There is also the problem of vanishing energy denominator. Here, we only consider the LF Yukawa model without a massless particle, so that we may avoid this problem by $-i\epsilon$ in denominators. If there is a massless particle like in QCD, we must be attentive to it.

We proved here that the effective Hamiltonian can be written in terms of G to the fourth order by the explicit calculation. But the general proof for higher orders is lacking. Although we do not know how the general proof goes, we think that it is likely that this feature persists to all orders. Recently Hansper proposed a nonperturbative approach for the FSTO's method in LF field theory.¹⁵⁾ Although he applied it only to the parton distributions, it is very useful to solve the mesonic bound states in QCD if it is applicable to our method.

In Appendix B, when the coupling constant is large enough, the lowest-energy state has the positive binding energy in the numerical calculation, but we do not regard it as a bound state because it depends on the transverse cutoff Λ_{\perp} . As mentioned above, our method is valid in small coupling and we expect that it is improved in higher order calculations. We are now extending the present work to the next order in order to confirm the cancellation of the cutoff dependence and to get bound states.¹²⁾

It is interesting to note that this method might also be applied to the similarity transformation in momentum space because Eq. (3.13) does not depend on the choice of η . If so, to get the effective Hamiltonian would be much easier than the traditional way.

Acknowledgement

The author is grateful to K. Harada for helpful discussions and encouragement, and also thanks A. Okazaki for his useful work.

Appendix A

— Light-Front Yukawa model —

In the LF framework, we use $x^+ = (x^0 + x^3)/\sqrt{2}$ as a time variable instead of t . The Lagrangian of the this model is

$$\mathcal{L} = \frac{1}{2}\partial_\mu\phi\partial^\mu\phi - \frac{1}{2}\mu^2\phi^2 + \bar{\psi}(i\gamma^\mu\partial_\mu - m + ig\gamma_5\phi)\psi. \quad (\text{A}\cdot 1)$$

By LF quantization with Dirac's quantization method, dynamical fields must satisfy the following commutation relations

$$[\phi(x), \partial_- \phi(y)]_{x^+=y^+} = \frac{i}{2}\delta(x^- - y^-)\delta^2(x_\perp - y_\perp), \quad (\text{A}\cdot 2)$$

$$\{\xi(x), \xi^\dagger(y)\}_{x^+=y^+} = \frac{1}{\sqrt{2}}\delta(x^- - y^-)\delta^2(x_\perp - y_\perp)\Lambda_+, \quad (\text{A}\cdot 3)$$

where $\xi(x)$ is the dynamical part of the fermion field $\psi(x)$:

$$\xi(x) = \Lambda_+\psi(x). \quad (\text{A}\cdot 4)$$

Λ_\pm are the projection operators of the fermion field and defined as

$$\Lambda_\pm = \frac{1}{\sqrt{2}}\gamma^0\gamma^\pm. \quad (\text{A}\cdot 5)$$

From Eq. (A.1), the familiar Legendre transformation gives the LF Hamiltonian

$$H = P^- = H_0 + H', \quad (\text{A}\cdot 6)$$

where

$$H_0 = \int dx^- d^2x_\perp \left\{ \frac{1}{2}(\partial_\perp\phi)^2 + \frac{1}{2}\mu^2\phi^2 + \xi^\dagger \frac{-\partial_\perp^2 + m^2}{\sqrt{2}i\partial_-} \xi \right\}, \quad (\text{A}\cdot 7)$$

$$H' = \int dx^- d^2x_\perp \left\{ -ig \left[\xi^\dagger \gamma^0 \gamma_5 \phi \frac{1}{\sqrt{2}i\partial_-} (i\alpha_\perp \cdot \partial_\perp + m\beta)\xi - \text{h.c.} \right] + \frac{g^2}{2} \left[(\xi^\dagger \phi) \frac{1}{\sqrt{2}i\partial_-} (\phi\xi) - \frac{1}{\sqrt{2}i\partial_-} (\phi\xi^T)(\xi^*\phi) \right] \right\}, \quad (\text{A}\cdot 8)$$

and

$$\alpha_{\perp} = \gamma^0 \gamma_{\perp}, \quad \beta = \gamma^0. \quad (\text{A}\cdot 9)$$

In the interaction picture, they become

$$H_0(x^+) = \int dx^- d^2 x_{\perp} \left\{ \frac{1}{2} (\partial_{\perp} \phi)^2 + \frac{1}{2} \mu^2 \phi^2 + \bar{\psi} \gamma^+ \frac{-\partial_{\perp}^2 + m^2}{2i\partial_-} \psi \right\}, \quad (\text{A}\cdot 10)$$

$$H'(x^+) = \int dx^- d^2 x_{\perp} \left\{ -ig\bar{\psi}\gamma_5\phi\psi + \frac{g^2}{2} \left[\bar{\psi}\phi \frac{\gamma^+}{2i\partial_-} (\phi\psi) - \left(\frac{\gamma^+}{2i\partial_-} \phi\psi \right)^{\text{T}} (\bar{\psi}\phi)^{\text{T}} \right] \right\} \\ + H_{\text{CT}}(x^+), \quad (\text{A}\cdot 11)$$

where all the field operators are defined in this picture. Note that $\psi(x)$ is not the one in Eq. (A.1) but a new field made from $\xi(x)$ in this picture, and the solution of the free Dirac equation:¹⁶⁾

$$\psi(x) = \left[1 + \frac{1}{\sqrt{2}i\partial_-} (i\alpha_{\perp} \cdot \partial_{\perp} + m\beta) \right] \xi(x). \quad (\text{A}\cdot 12)$$

$H_{\text{CT}}(x^+)$ is the part which corresponds to the usual counterterms obtained by shifting the parameters.

We assume that the LF diagrams are equivalent to the covariant ones. More concretely, in the LF framework the fermion propagator

$$S_F(k) = \int d^4x \langle 0 | \text{T}^+ (\psi(x) \bar{\psi}(0)) | 0 \rangle e^{ik \cdot x} = \frac{i}{\not{k} - m + i\epsilon} - \frac{i}{2k^+} \gamma^+, \quad (\text{A}\cdot 13)$$

includes the noncovariant term. But in the first two diagrams in Fig. 7, the contributions from the second term are naively canceled by the vertex

$$-ig^2 \gamma^+ \left\{ \frac{1}{2(k_1^+ + q_1^+)} + \frac{1}{2(k_1^+ - q_2^+)} \right\} \quad (\text{A}\cdot 14)$$

in the last diagram in Fig. 7, which comes from the instantaneous interaction in the Hamiltonian. Therefore, we regard the fermion propagator as the first term in Eq. (A.13) and covariant effectively, and omit the second term in Eq. (A.13) and the vertex Eq. (A.14) together. As a result, the scalar and fermion propagator are given by

$$\Delta_F(q) = \frac{i}{q^2 - \mu^2 + i\epsilon}, \quad (\text{A}\cdot 15)$$

$$S_F(k) = \frac{i}{\not{k} - m + i\epsilon}. \quad (\text{A}\cdot 16)$$

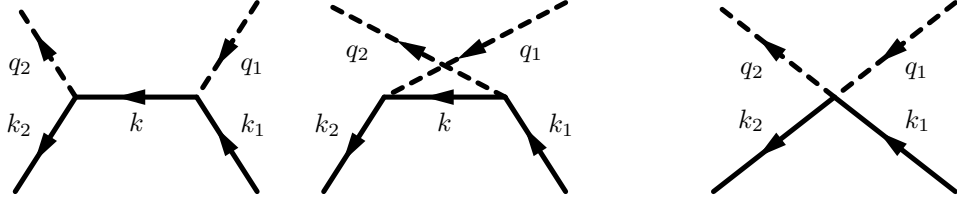


Fig. 7. The first two diagrams are examples which include an internal fermion line. The propagators include the noncovariant term. The last diagram is the contribution from the instantaneous vertex included in the LF Hamiltonian.

Appendix B

— *Explicit calculations and numerical result* —

We calculate the ground state energy numerically to the second order in g . Of course, the calculations to this order are not so different from the other methods;¹⁷⁾ the advantage of the present formulation becomes apparent in the higher orders.¹²⁾ The reason why we present the second order calculation here is to demonstrate some features of our method and to clarify what would be expected in the next order.

From Eqs. (3.13) and (3.20), the LF effective Hamiltonian is

$$H_{\text{eff}} = \frac{1}{2}\eta(H_0 + \mathcal{G}_2)\eta + \text{h.c.} + \mathcal{O}(g^4) \quad (\text{B}\cdot 1)$$

to g^2 order. Also, we add the flavor of fermions. It is easy to estimate Eq. (B.1) from Feynman diagrams by using our rules.

Since possible graphs are the same as those needed in constructing the S-matrix, we can immediately imagine those which contribute to Eq. (B.1). The Feynman diagrams associated with the effective Hamiltonian to the second order are shown in Fig. 8.

Terms which should be renormalized are only fermion self-energy terms \mathcal{M}_2 and $\bar{\mathcal{M}}_2$ in this order. Although we do not give the rules for those, they are much the same as those for \mathcal{V}_n . The self-energy terms correspond to the first and the third graphs in the second line of Fig. 8 and are written as

$$\begin{aligned} \mathcal{G}_2^{\text{self}} = & -\sum_{\lambda} \int_{p_1} \int_{p_2} (p_1^- - p_2^-) \int_{-\infty}^{\infty} \frac{dk^-}{2\pi} \left(\frac{-i}{p_1^- - k^- - i\epsilon} \right) \left(\frac{-i}{k^- - p_2^- - i\epsilon} \right) \\ & \times \bar{u}_i(p_1, \lambda) \left\{ \int \frac{d^4q}{(2\pi)^4} \Delta_F(q) (-g\gamma_5) S_{F_i}(k-q) (-g\gamma_5) \right. \\ & \quad \left. + [(1 - Z_{2i})^{(2)} S_{F_i}^{-1}(k) - i\delta m_i^{(2)}] \right\} u_i(p_2, \lambda) \\ & \times \eta b_{i\lambda}^{\dagger}(p_1) b_{i\lambda}(p_2) \eta (2\pi)^3 \delta(p_1 - p_2), \end{aligned} \quad (\text{B}\cdot 2)$$

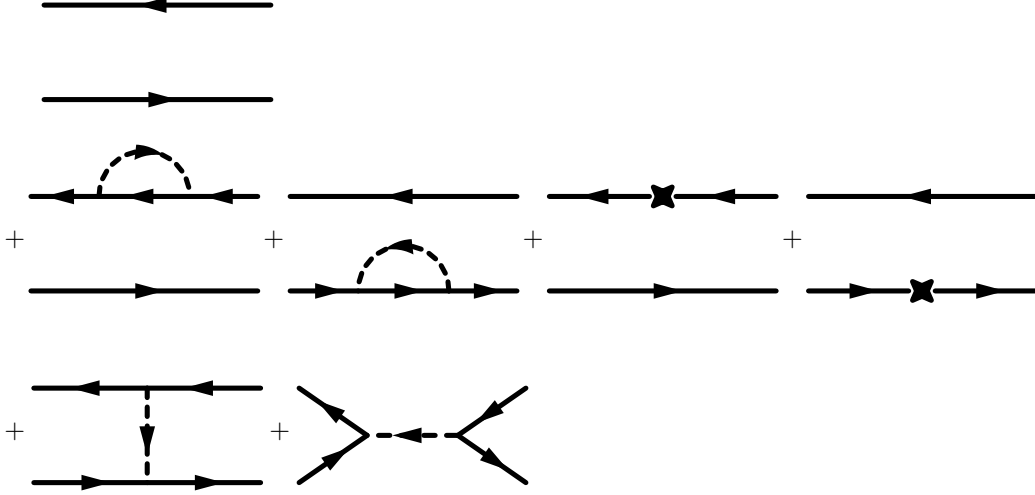


Fig. 8. Feynman diagrams which are necessary to construct the effective Hamiltonian to the second order in g . The first diagram is the free part. The next four diagrams are self-energy parts and X mean the counterterms for the fermion mass and field. The last two diagrams are the one-scalar-exchange part and the fermion annihilation part.

where $\delta m_i^{(2)}$'s and $(1 - Z_{2i})^{(2)}$'s are the masses and field renormalization constants of order g^2 respectively, and the on-shell condition ($p_1^2 = p_2^2 = m_i^2$) for the external fermion lines is satisfied. Although there is no energy conserving delta function, $p_1^- = p_2^-$ is satisfied due to $p_1^+ = p_2^+$, $p_{1\perp} = p_{2\perp}$ and the on-shell condition. Therefore

$$\begin{aligned}
& -(p_1^- - p_2^-) \left(\frac{-i}{p_1^- - k^- - i\epsilon} \right) \left(\frac{-i}{k^- - p_2^- - i\epsilon} \right) \\
&= \frac{1}{p_1^- - k^- - i\epsilon} + \frac{1}{k^- - p_1^- - i\epsilon} \\
&= 2\pi i \delta(p_1^- - k^-).
\end{aligned} \tag{B.3}$$

This is what is said in the beginning of Sec. 3.3.1. Integrating k^- , we obtain

$$\mathcal{G}_2^{\text{self}} = \sum_i \sum_\lambda \int_p \frac{1}{2p^+} \bar{u}_i(p, \lambda) \Sigma_i^{(2)}(p) u_i(p, \lambda) \eta b_{i\lambda}^\dagger(p) b_{i\lambda}(p) \eta, \tag{B.4}$$

where

$$\Sigma_i^{(2)}(p) = i \int \frac{d^4 q}{(2\pi)^4} \Delta_F(q) (-g\gamma_5) S_{Fi}(p-q) (-g\gamma_5) + \delta m_i^{(2)}, \tag{B.5}$$

and $p^2 = m_i^2$. The counterterm for the fermion field in Eq. (B.5) vanishes by using the Dirac equation. Obviously, $\Sigma_i^{(2)}(p)$ is the same as fermion self-energy terms in the covariant perturbation theory. It is convenient to impose the physical renormalization condition

$$\bar{u}_i(p, \lambda) \Sigma_i^{(2)}(p) u_i(p, \lambda) = 0 \quad (p^2 = m_i^2), \tag{B.6}$$

in order for the fermion masses to be the physical one. For anti-fermion, the same argument is applied.

The rest are the scalar exchange part and the fermion annihilation part which are represented by the last two graphs in Fig. 8. After integrating the energies, we obtain

$$\begin{aligned}
\mathcal{G}_2^{\text{ex}} + \mathcal{G}_2^{\text{ex}\dagger} &= g^2 \sum_{\lambda_1} \sum_{\lambda_2} \sum_{\sigma_1} \sum_{\sigma_2} \int_{p_1} \int_{p_2} \int_{l_1} \int_{l_2} (2\pi)^3 \delta^3(p_1 + l_1 - p_2 - l_2) \\
&\quad \times \bar{u}_i(p_1, \lambda_1) \gamma_5 u_i(p_2, \lambda_2) \bar{v}_j(l_2, \sigma_2) \gamma_5 v_j(l_1, \sigma_1) \\
&\quad \times \left[\frac{1}{(p_1 - p_2)^2 - \mu^2} + \frac{1}{(l_2 - l_1)^2 - \mu^2} \right] \\
&\quad \times \eta b_{i\lambda_1}^\dagger(p_1) d_{j\sigma_1}^\dagger(l_1) d_{j\sigma_2}(l_2) b_{i\lambda_2}(p_2) \eta
\end{aligned} \tag{B.7}$$

$$\begin{aligned}
\mathcal{G}_2^{\text{an}} + \mathcal{G}_2^{\text{an}\dagger} &= -g^2 \sum_{\lambda_1} \sum_{\lambda_2} \sum_{\sigma_1} \sum_{\sigma_2} \int_{p_1} \int_{p_2} \int_{l_1} \int_{l_2} (2\pi)^3 \delta^3(p_1 + l_1 - p_2 - l_2) \\
&\quad \times \bar{u}_i(p_1, \lambda_1) \gamma_5 v_i(l_1, \sigma_1) \bar{v}_i(l_2, \sigma_2) \gamma_5 u_i(p_2, \lambda_2) \\
&\quad \times \left[\frac{1}{(p_1 + l_1)^2 - \mu^2} + \frac{1}{(p_2 + l_2)^2 - \mu^2} \right] \\
&\quad \times \eta b_{i\lambda_1}^\dagger(p_1) d_{i\sigma_1}^\dagger(l_1) d_{i\sigma_2}(l_2) b_{i\lambda_2}(p_2) \eta,
\end{aligned} \tag{B.8}$$

which are all the second order interactions in the LF effective Hamiltonian. Of course, since it does not have the particle-number-changing interactions, the eigenstate is a pure two-body state.

We set the total transverse momentum P_\perp to 0 for simplicity. The eigenstate may be written as

$$\begin{aligned}
|\Psi_{ij}(P^+, m)\rangle &= \sum_{\lambda_1} \sum_{\lambda_2} \int_0^1 dx \int_0^\infty d\kappa \int_0^{2\pi} d\varphi \frac{1}{2(2\pi)^3} \sqrt{\frac{\kappa}{x(1-x)}} \\
&\quad \times e^{i(m-\lambda_1/2-\lambda_2/2)\varphi} \Psi_{ij}(x, \kappa; \lambda_1, \lambda_2, m) b_{i\lambda_1}^\dagger(p_1) d_{j\lambda_2}^\dagger(p_2) |0\rangle,
\end{aligned} \tag{B.9}$$

where

$$p_1^+ = xP^+, \quad p_2^+ = (1-x)P^+, \quad (p_{1\perp} - p_{2\perp})/2 = \kappa_\perp, \tag{B.10}$$

$$\kappa = |\kappa_\perp|, \quad \tan \varphi = \frac{\kappa_\perp^2}{\kappa_\perp^1}. \tag{B.11}$$

m is the eigenvalue of the third component of the total angular momentum J_3 . In the LF coordinates, the squared total angular momentum \mathbf{J}^2 is not a good quantum number, but the third component J_3 , the helicity, is.

We discretized x with L equally-spaced points, in the numerical calculations of diagonalization. We put a transverse cutoff Λ_\perp for κ and, also used the following variable

$$z = \left(\frac{\kappa}{\Lambda_\perp} \right)^{1/3}, \tag{B.12}$$

instead of κ and discretized z with N equally-spaced points because the wavefunctions are sharp for $\kappa \sim 0$, but flat for $\kappa \sim \Lambda_\perp$.

The results are shown in Fig. 9 and Fig. 10. We set the parameters $L = 10$, $N = 30$, $m = 0$, the fermion mass $m_1 = 1.0$ GeV, the anti-fermion mass $m_2 = 1.0$ GeV and the scalar mass $\mu = 0.01$ GeV in all the cases. We define $\alpha_g = g^2/4\pi$.

Fig. 9 shows α_g dependence of the binding energy of the ground state for various transverse cutoff Λ_\perp . (a) is the case that the fermion flavor is different from the anti-fermion one, that is, excluding the fermion annihilation part. (b) is the case of including it. In (a), the binding energy is almost independent of Λ_\perp in $\alpha_g < 1.5$, but the ground state is not a bound state because it is slightly negative. Even though the binding energy becomes positive and larger as α_g grows, we can not say that the ground state is bound because it apparently depends on Λ_\perp for large α_g . This means that the binding energy depends on Λ_\perp even if α_g is small. If we consider the perturbation theory of the effective Hamiltonian, which treats $\eta(\mathcal{G}_2 + \mathcal{G}_2^\dagger)\eta/2$ as the interaction, with small α_g , the leading term of the eigenvalue which depends on the cutoff corresponds to Eq. (3.60) times (-1) . As mentioned in Sec. 3.4, we expect that the dependence on Λ_\perp is weakened in the next order calculation. (b) has stronger dependence on Λ_\perp than (a).

Fig. 10 shows Λ_\perp dependence of the binding energy of the ground state for $g = 3$ with the fermion annihilation part. The reason for its behavior is *not* that the LF effective Hamiltonian needs the renormalization of the scalar mass which corresponds to a fermion loop. The perturbative analysis shows that the fourth order term of the eigenvalue is logarithmically divergent like in Eq. (3.60). We consider that it is canceled by adding the fourth order terms.

Appendix C

— Ambiguity in the integration —

In this appendix, we explain that there is in general an ambiguity in the integrations like that appearing in Eq. (3.46) by demonstrating an explicit example. Let us consider the following integration:

$$I = \lim_{\Lambda_1 \rightarrow \infty} \lim_{\Lambda_2 \rightarrow \infty} \int_{-\Lambda_1}^{\Lambda_1} \frac{dq_1^-}{2\pi} \int_{-\Lambda_2}^{\Lambda_2} \frac{dq_2^-}{2\pi} \frac{-i}{k_1^- - q_1^- - i\epsilon} q_1^- \frac{i}{q_1^- - q_2^- - i\epsilon} \frac{-i}{q_2^- - k_2^- - i\epsilon}. \quad (\text{C.1})$$

If k_1^- and k_2^- are finite, we can take the integration contours which have a infinite radius in the lower half plane for q_1^- and in the upper one for q_2^- respectively. By the residue theorem, I becomes

$$I = \frac{k_1^- + k_2^-}{2} \frac{i}{k_1^- - k_2^- - i\epsilon} - \lim_{\Lambda_1 \rightarrow \infty} \lim_{\Lambda_2 \rightarrow \infty} i \int_0^{-\pi} \frac{d\theta_1}{2\pi} \int_0^\pi \frac{d\theta_2}{2\pi} \frac{1}{1 - \frac{\Lambda_2}{\Lambda_1} e^{i(\theta_2 - \theta_1)}}, \quad (\text{C.2})$$

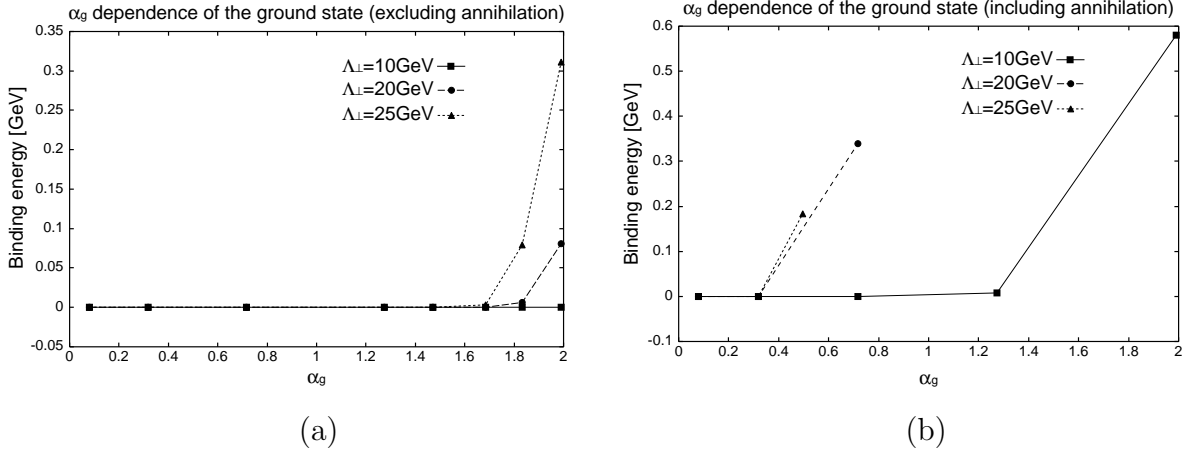


Fig. 9. α_g dependence of the binding energy of the ground state for various Λ_\perp . α_g is defined as $g^2/4\pi$. The calculations are done for $L = 10$, $N = 30$, $m = 0$, $m_1 = m_2 = 1.0$ GeV, and $\mu = 0.01$ GeV. (a) is the case of excluding the fermion annihilation part and (b) is the case of including it.

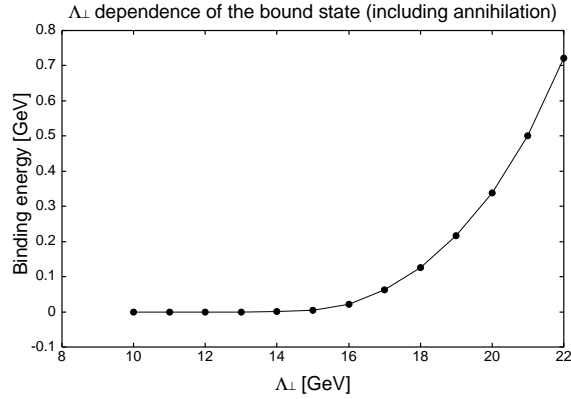


Fig. 10. Λ_\perp dependence of the binding energy of the ground state including the fermion annihilation part. The calculations are done for $L = 10$, $N = 30$, $\alpha_g = 0.716$, $m = 0$, $m_1 = m_2 = 1.0$ GeV, and $\mu = 0.01$ GeV.

where we keep the radii finite in the second term because I have various values depending on ways to take the limits. For example,

1. $\Lambda_1 \rightarrow \infty$ before $\Lambda_2 \rightarrow \infty$,

$$I = \frac{k_1^- + k_2^-}{2} \frac{i}{k_1^- - k_2^- - i\epsilon} + \frac{i}{4}. \quad (\text{C}\cdot 3)$$

2. $\Lambda_2 \rightarrow \infty$ before $\Lambda_1 \rightarrow \infty$,

$$I = \frac{k_1^- + k_2^-}{2} \frac{i}{k_1^- - k_2^- - i\epsilon}. \quad (\text{C}\cdot 4)$$

3. $\Lambda_1 = \Lambda_2 \rightarrow \infty$,

$$I = \frac{k_1^- + k_2^-}{2} \frac{i}{k_1^- - k_2^- - i\epsilon} + \frac{i}{8}. \quad (\text{C}\cdot 5)$$

The other limits may yield the other constants. Note that such ambiguity arises from the terms whose total dimension of the variables of the integrations is zero.

References

- [1] I. Tamm, J. Phys. (Moscow) **9**, 449 (1945); S. M. Dancoff, Phys. Rev. **78** (1950), 382.
- [2] R. J. Perry, A. Harindranath, and K. G. Wilson, Phys. Rev. Lett. **65** (1990), 2959.
- [3] S. D. Glazek and K. G. Wilson, Phys. Rev. D **48** (1993), 5863; Phys. Rev. D **49** (1994), 4214.
- [4] F. Wegner, Ann. Physik. **3** (1994), 77.
- [5] M. Brisudová and R. J. Perry, Phys. Rev. D **54** (1996), 1831; M. Brisudová, R. J. Perry, and K. G. Wilson, Phys. Rev. Lett. **78** (1997), 1227.
- [6] K. G. Wilson, T. S. Walhout, A. Harindranath, W. M. Zhang, R. J. Perry and S. D. Glazek, Phys. Rev. D **49** (1994), 6720; R. J. Perry, in *Hadron Physics 94*, edited by V. E. Herscovitz, C. Vasconcellos, (World Scientific, Singapore, 1995).
- [7] W. M. Zhang, Phys. Rev. D **56** (1997), 1528; E. L. Gubankova and F. Wegner, Phys. Rev. D **58** (1998), 025012; B. H. Allen and R. J. Perry, Phys. Rev. D **58** (1998), 125017; S. D. Glazek, Acta Phys. Pol. B **29** (1998), 1979.
- [8] K. Harada and A. Okazaki, Phys. Rev. D **55** (1997), 6198.
- [9] M. Taketani, S. Machida, and S. Onuma, Prog. Theor. Phys. **7** (1952), 45.
- [10] N. Fukuda, K. Sawada, and M. Taketani, Prog. Theor. Phys. **12** (1954), 156; K. Inoue, S. Machida, M. Taketani, and T. Toyoda, Prog. Theor. Phys. **15** (1956), 122.
- [11] S. Okubo, Prog. Theor. Phys. **12** (1954), 603.
- [12] Y. Yamamoto, in progress.
- [13] S. D. Glazek, A. Harindranath, S. Pinsky, J. Shigemitsu, and K. G. Wilson, Phys. Rev. D **47** (1993), 1599.
- [14] See, e.g., S. Weinberg, *The Quantum Theory of Fields Volume II Modern Applications* (Cambridge University Press, Cambridge, 1996), p. 256.
- [15] J. Hansper, Phys. Rev. D **62** (2000), 056001.
- [16] S. J. Brodsky, H. C. Pauli, and S. S. Pinsky, Phys. Rep. **301** (1998), 299.
- [17] A. Okazaki, “Perturbative renormalization in the light-front Hamiltonian approach”, Ph. D. Thesis.